Determination of Liquid/Gas Interface and Liquid Center of Gravity for GPM Tank with PMD Using Surface Evolver

David J. Benson[1]
NASA Goddard Space Flight Center, Greenbelt, MD, 20771

Many spacecraft, such as the Global Precipitation Mission (GPM) spacecraft, use propellant management devices (PMDs) to control liquid propellant within propellant tanks. Surface Evolver, an energy minimization routine, is used to find liquid-gas interface shapes due to surface tension and propellant center of mass locations for varying initial liquid positions, contact angles, and fill fractions for the GPM tank with a PMD. This study shows that Surface Evolver can accurately model the liquid-gas interface and liquid center of mass location for a complicated tank and PMD. The Surface Evolver results show that the initial position of the propellant, the contact angle between the propellant and solid surfaces, and the fill fraction of the propellant can drastically affect the liquid-gas interface in the tank and thus the center of mass of the propellant.

Nomenclature

a	=	lower integration limit along revolve axis
A_{ds}	=	dry surface area
A_{fs}	=	\surface area if liquid-gas interface, also referred to as the free surface
A_T	=	total surface area of tank
A_{ws}	=	wet surface area
b	=	upper integration limit along revolve axis
cf	=	local circumference of the circle which is perpendicular to the z-axis
cm_x	=	x-component of propellant center of mass
cm_y	=	y-component of propellant center of mass
cm_z	=	z-component of propellant center of mass
$d\vec{A}$	=	differential area of facet
Δsa_{bottdx}	=	differential surface area equation in the x-direction for bottom of sphere
Δsa_{bottdy}	=	differential surface area equation in the y-direction for bottom of sphere
Δsa_{topdx}	=	differential surface area equation in the x-direction for top of sphere
Δsa_{topdy}	=	differential surface area equation in the y-direction for top of sphere
E	=	potential energy due to gravity for the propellant
E_T	=	total energy due to surface tension
γ_{lg}	=	liquid-gas surface tension
γ_{ls}	=	liquid-solid surface tension
γ_{sg}	=	solid-gas surface tension
h	=	liquid climb height along the tank wall from center of tank (origin)
$\vec{i}$	=	unit vector in x-direction
$\vec{j}$	=	unit vector in y-direction
$\vec{k}$	=	unit vector in z-direction
ρ	=	density of propellant
S_{area}	=	surface area of revolved surface
$S_{areabott}$	=	surface area of bottom half of sphere
$S_{areabottfunc}$	=	surface area of wetted section of bottom part of the sphere as a function of h
$S_{areatop}$	=	surface area of top half of sphere
$S_{areatopfunc}$	=	surface area of wetted section of top part of the sphere as a function of h

[1] Aerospace Engineer, Propulsion Branch, GSFC Mailstop: 597, Greenbelt, MD, 20771, and AIAA Member

θ	=	contact angle as measured from the solid to liquid surfaces through the liquid volume
V	=	volume of propellant
x	=	coordinate in the x-direction
y	=	coordinate in the y-direction
z	=	coordinate in the z-direction

I. Introduction

KNOWING the center of mass of the liquid propellant is important for attitude control, especially for spacecraft which have a large wet/dry mass ratio and/or spacecraft that have large thrusters that can exert large moments on the spacecraft. Knowledge of the liquid/gas interface is important for identifying if the outlet areas of the tank will be wetted after maneuvers and when using thermal capacitance models to gauge propellant during flight. On earth, gravity causes a flat liquid/gas interface to be created in a propellant tank. The liquid/gas interface formed in microgravity is caused by surface tension. This results in unintuitive liquid/gas interface shapes, especially when a vane-type propellant management device (PMD) is used to orient the propellant at the exit of the tank.

Surface Evolver[1] is an energy minimization routine that can be used to model the steady-state liquid-gas interface and liquid center of mass position within propellant tanks.[2-7] The energies for propellant tanks can include surface tension energy and potential energy (body accelerations). Surface Evolver only models the liquid surface, and hence converges quickly in most cases. Surface Evolver was developed by Ken Brakke, circa 1991, as part of the Geometry Supercomputing Project, which was funded by different academic, government, and private entities.[8] It is provided free of charge, with adequate documentation provided by Ken Brakke. Several good review papers exist that summarize the work done with Surface Evolver as applicable to propellant tank and PMD design.[9-12]

This paper will present methods and results for calculating the liquid-gas interface and liquid center of mass for the propellant in the Global Precipitation Mission (GPM) tank with a slightly simplified version of the GPM propellant management device (PMD). The liquid initial position in the tank, contact angle between the liquid and solid surfaces, and the liquid fill fraction were varied to give a complete view of how the liquid will behave after maneuvers.

II. Background

A. Geometry and Terms

Figure 1 shows the PMD with its various parts called out. Figure 2 shows the GPM tank and PMD with the axes used for this paper. The blue lines outline the tank wall and the red lines outline the PMD.

The following terms are defined as used in this paper: contact angle, free surface, liquid initial position, Bond number, body acceleration, and directions associated with axes.

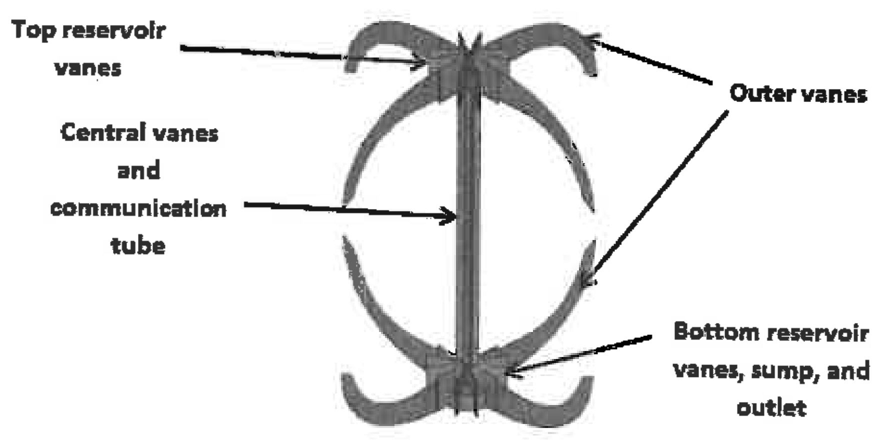

Figure 1. GPM PMD with different parts labeled.

The contact angle is the angle formed between a liquid and solid. When this angle is large, the solid surface is considered to be non-wetting. When this angle is small, the solid surface is considered to be wetting. A zero degree contact angle is considered to be perfectly wetting.

The free surface is the interface between the liquid and gas in the tank.

The liquid initial position is defined as the location of the liquid when a simulation is begun. Physically, this is the liquid position once a spacecraft maneuver has ended and all sloshing has stopped (or nearly so).

The Bond number (Bo) is a non-dimensional term used to compare the relative effect of surface tension and a body acceleration. If the Bond number is much smaller than 1, the surface tension is the dominant fluid force. If the Bond number is much greater than 1, the body acceleration becomes the dominant force. The body acceleration on earth is gravity, but in space it is the acceleration caused by the spacecraft accelerating or rotating in a specific direction.

The directions used for this paper are up, down, left, right, forward, and back. Up is in the positive z-direction, right is in the positive y-direction, and forward is in the positive x-direction, with the opposites of these terms being in the opposite direction along the same axis.

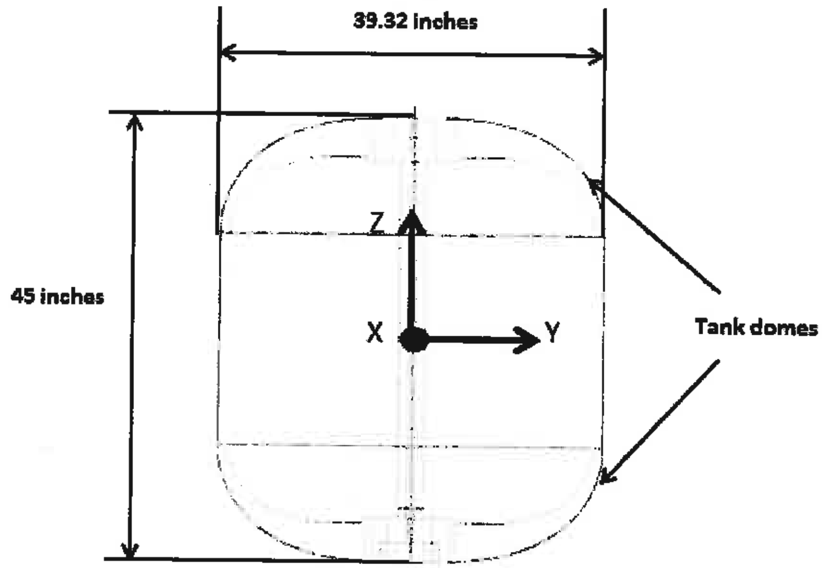

Figure 2. GPM Tank and PMD showing tank dimensions and axes used in this paper.

B. Low-Gravity Fluid Theory

The absence of significant body accelerations during much of the spacecraft flight results in surface tension forces dominating fluid flow (low Bond number). The lack of body accelerations allows the propellant to be modeled by only looking at surface tension. Because surface tension dominates the fluid behavior in this problem, a brief review of the equations for calculating the energy associated with surface tension is beneficial to understand the results presented in this paper.

Surface tension is an interaction between different states of matter. There is a liquid-solid surface tension, γ_{ls}, a solid-gas surface tension, γ_{sg}, and a liquid-gas surface tension, γ_{lg}. Equation (1)[13] shows how the different types of surface tension relate in a physical system when the contact angle, θ, is known.

$$\gamma_{sg} - \gamma_{ls} = \gamma_{lg} \cos\theta \tag{1}$$

Surface tension is measured in N/m in SI units and can be considered an energy density. Equation (2) shows how energy per surface area J/m^2 is equivalent to N/m where J is Joules, m is meters, and N is newtons. It is because of this relation that sometimes the various surface tensions are referred to as surface energies; however, for this paper the term surface tension will be used.

$$\frac{J}{m^2} = \frac{kg{\cdot}m^2}{s^2{\cdot}m^2} = \frac{N}{m} \tag{2}$$

The energy in a propellant tank problem due to surface tension, E_T, can be represented by multiplying the surface tensions in Eq. (1) by the surface area with which each surface tension is associated. The different surface areas are dry surface area, A_{ds}, wetted surface area, A_{ws}, and free surface area, A_{fs}. Equation (3) shows the final the result.

$$E_T = A_{ds}\gamma_{sg} + A_{ws}\gamma_{ls} + A_{fs}\gamma_{lg} \tag{3}$$

By noting that the total surface area, A_T, of the tank is a constant, we can replace either the dry surface area or the wetted surface area in Eq. (3) with a term involving the total surface area. The relation between the surface areas is shown in Eq. (4).

$$A_{ws} = A_T - A_{ds} \tag{4}$$

By substituting Eq. (1) and Eq. (4) into Eq. (3) and rearranging terms, Eq. (5) is obtained.

$$E_T = A_{ds}\gamma_{lg}\cos\theta + A_{fs}\gamma_{lg} + A_T\gamma_{ls} \tag{5}$$

The surface tensions and total surface area of the tank are constants, so the term, $A_T\gamma_{ls}$, in this problem can be ignored when doing an energy minimization. Equation (5) is the equation used in Surface Evolver when modeling a zero degree contact angle. This is because A_{ds} gives the same contribution as A_{fs} due to the cosine term equaling one.

By rearranging terms in Eq. (4), and then plugging the result into Eq. (3), Eq. (6) is obtained.

$$E_T = -A_{ws}\gamma_{la}\cos\theta + A_{fs}\gamma_{la} + A_T\gamma_{sa} \tag{6}$$

As with Eq. (5), the surface tensions and total area are constant and so the term, $A_T\gamma_{sa}$, is ignored when Equation (6) is used in to find the energy minimum in Surface Evolver.

C. Method for Calculating Surface Energies

Surface Evolver automatically calculates the free surface area, and with some user programming, can be made to calculate the wetted or dry surface area.

In the case of a zero degree contact angle, the dry surface area has the same energy density as the free surface area and so there is no need to program in the dry surface area. Instead, the gas bubble is modeled. When the bubble touches, or "dries out" the tank wall, Surface Evolver calculates the surface area of the bubble facet, and therefore, the dry surface area. All surfaces which are not touched by the air bubble are considered wetted. Since Eq. (5) does not explicitly contain this quantity it is not important for the calculation of the total energy.

The wetted or dry surface area needs to be calculated explicitly within Surface Evolver for non-zero degree contact angles. The wetted surface area is calculated for the cases presented in this paper since Eq. (6) is used to calculate the total energy. For simple shapes, such as spheres, cylinders, and hemispheres, the calculation of the wetted area through a line integral along the three phase boundary is straight forward. The example of a sphere can be found in the Surface Evolver manual.[1]

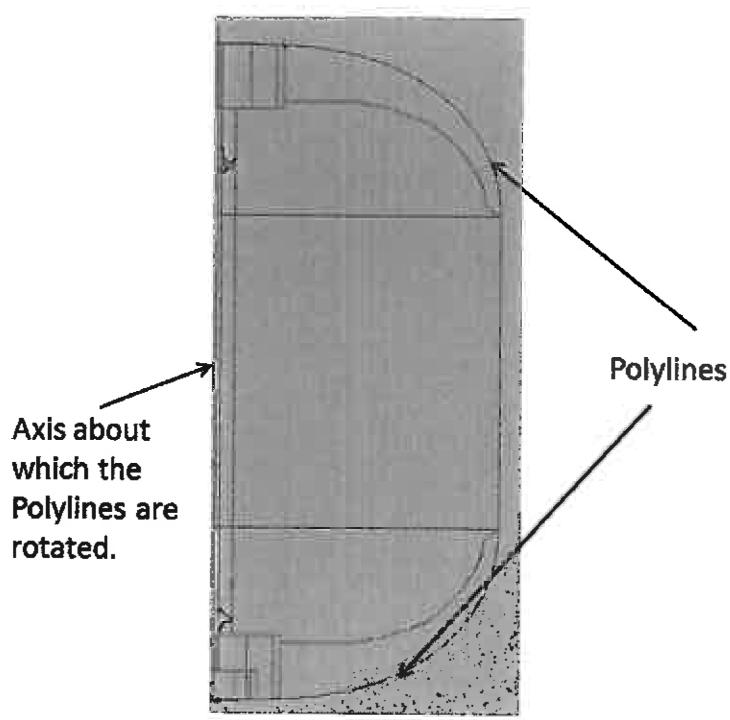

Figure 3. Polylines that make up the GPM tank outline and axis about which the polylines are rotated to create GPM tank surface.

GPM uses a cylindrical tank with isotensoid domes. The shape of the isotensoid domes is described within Surface Evolver by seven curves that make up a polyline. This polyline is then revolved around the axis that runs down the center of the tank. The polylines and rotation axis are shown in Figure 3.

To illustrate the method used to calculate the wetted energy of the tank wall, and to keep the illustration reasonably simple, the example of a sphere is used. Even though the sphere's wetted surface area can be obtained as shown in the Surface Evolver manual, it provides a good example of the method used to find the wetted surface area in the GPM tank due to the simplicity of its shape. The sphere is shown in Figure 4 below with the origin of the coordinate system at the center of the tank. The sphere has a radius of 1.

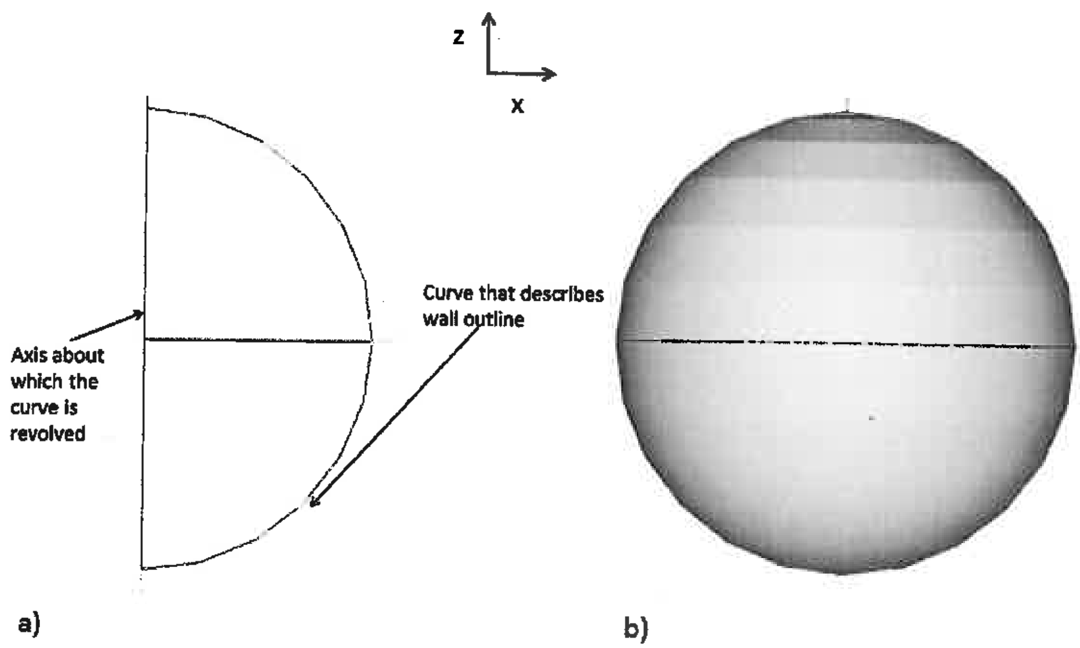

Figure 4. Drawing showing the a) curve which is revolved and the b) resulting sphere.

Step 1 involves calculating the surface area of a revolve of the polyline that describes the outline of the tank wall. Note: this step can be ignored if an equation already exists for the surface area of the tank shape, such as with a sphere, but for demonstration purposes we will show the step here. Calculating the surface area, S_{area}, of a revolve can be done through Eq. (7)[14] where a and b are the lower and upper integration limits along the revolve axis, respectively.

$$S_{area} = \int_a^b 2\pi x \sqrt{1 + (\frac{dx}{dz})^2} dz \tag{7}$$

Equations (8) and (9) are the result when combining Equation (7) and the equation for the outline of the arc shown in Fig. 4. $S_{areabott}$ and $S_{areatop}$ are the surface areas for the bottom half of the sphere and the top half of the sphere, respectively. When the top and bottom areas are summed the known surface area of a sphere with a radius of 1, 4π, is found.

$$S_{areabott} = \int_{-1}^{0} 2\pi\sqrt{1-z^2} \sqrt{1 + (\frac{-z}{\sqrt{1-z^2}})^2} dz = 2\pi \tag{8}$$

$$S_{areatop} = \int_{0}^{1} 2\pi\sqrt{1-z^2} \sqrt{1 + (\frac{-z}{\sqrt{1-z^2}})^2} dz = 2\pi \tag{9}$$

Step 2 requires the defining of an equation that gives the local circumference, *cf*, of the tank as a function of distance along the rotation axis. For the purposes of this study the distance along the rotation axis, *h*, corresponds to the height to which the liquid climbs up the wall. Equation (10) shows the local circumference equation for a sphere.

$$cf = 2\pi\sqrt{(1-h)(1+h)} \tag{10}$$

Step 3 requires an equation that allows the calculation of the surface area given different liquid climb heights along the tank wall. This step involves modifying Eq. (8) and (9) so that the definite integral involves the extra variable, *h*. Equations (11) and (12) are the resulting equations where $S_{areabottfunc}$ and $S_{areatopfunc}$ are the equations used when the liquid climb height is below the z=0 plane or above z=0 plane, respectively.

$$S_{areabottfunc} = \int_{-1}^{h} 2\pi\sqrt{1-z^2}\sqrt{1+(\frac{-z}{\sqrt{1-z^2}})^2}dz = 2\pi h + 2\pi \tag{11}$$

$$S_{areatopfunc} = \int_{0}^{h} 2\pi\sqrt{1-z^2}\sqrt{1+(\frac{-z}{\sqrt{1-z^2}})^2}dz = 2\pi h \tag{12}$$

Both equations are valid at $h = 0$. It is important to note that if there are two separate pools of liquid, then the direction from which h is currently measured (bottom to top) would need to be switched (top to bottom) for the pool at the top of the tank, and hence, each pool would have a unique bottom and top.

Step 4 involves combining what has been done in the previous three steps to create equations that Surface Evolver can integrate. Figure 5 shows the differential surface area, Δsa, as a function of differential arc length, Δcf. Equations (13), (14), (15), and (16) show how all the information above will be put together. These equations give the differential area, Δsa, for the bottom and top integrated in the x and y directions. Δsa_{bottdx} is for the bottom part of the sphere in the x-direction, Δsa_{topdx} is for the top part of the sphere in the x-direction, $\Delta sa_{bottomdy}$ is for the bottom part of the sphere in the y-direction, and Δsa_{topdy} is for the top part of the sphere in the y-direction.

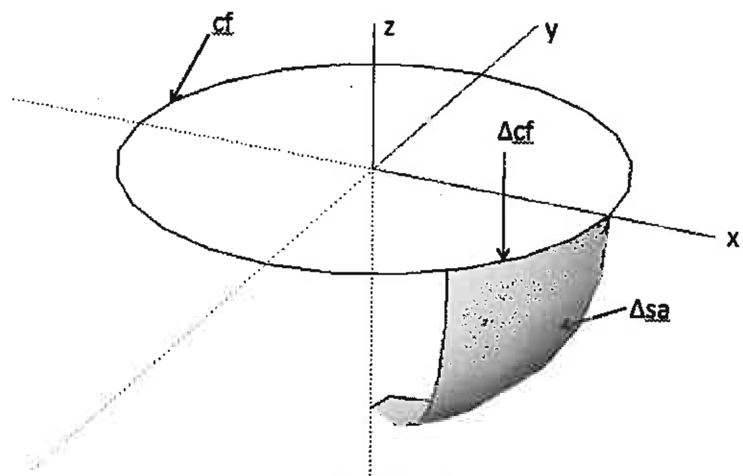

Figure 5. Figure showing Δsa and Δcf for the sphere.

$$\Delta sa_{bottdx} = \frac{y}{(x^2+y^2)}\sqrt{(1-h)(1+h)}\frac{1}{cf}(S_{areabottom}) \tag{13}$$

$$\Delta sa_{topdx} = \frac{y}{(x^2+y^2)}\sqrt{(1-h)(1+h)}\frac{1}{cf} * (S_{areatopfunc} + S_{areabott}) \tag{14}$$

$$\Delta sa_{bottdy} = \frac{-x}{(x^2+y^2)}\sqrt{(1-h)(1+h)}\frac{1}{cf}(S_{areabottfunc}) \tag{15}$$

$$\Delta sa_{topdy} = \frac{-x}{(x^2+y^2)}\sqrt{(1-h)(1+h)}\frac{1}{cf}(S_{areatopfunc} + S_{areabott}) \tag{16}$$

Surface Evolver will solve the equations for each edge that makes up the curve that marks the three phase boundary. It will then add up the results to give the final wetted surface area. In practice the surface area is a means of obtaining the surface energy. To convert Eq. (13), (14), (15), and (16) into energy equations, multiply them by the cosine of the contact angle in radians as explained in Section B.

D. Method for Calculating the Center of Mass

For spacecraft maneuvers, it is essential to know the center of mass of the propellant within a propellant tank. Surface Evolver can easily compute the center of mass of the propellant. This paper will not present a mathematically rigorous derivation of the method used, but will present the author's methodology for determining the correct way to compute the center of mass within Surface Evolver.

Starting with the equation used to calculate the potential energy due to gravity within Surface Evolver, Eq. (17)[1], it can be shown how to program Surface Evolver to find the center of mass location of the propellant. Equation (17) shows the equation for calculating gravitational potential energy, E, over a facet. The unit vector in the *z*-direction, $\vec{k}$, differential area, $d\vec{A}$, gravity acceleration, G, and density, ρ, are included in Eq. (17). Equation (18) shows a simplified version of Eq. 17 that includes the *z*-component of the center of mass, cm_z, and the volume, V, of the propellant.

$$E = G(\rho) \iint \frac{1}{2} z^2 \vec{k} \cdot d\vec{A} \tag{17}$$

$$E = G(\rho)(V)(cm_z) \tag{18}$$

A comparison of Eq. (17) and Eq. (18). shows that the propellant volume is included in the integral in Eq. (17). By dividing out V from the integral in Eq. (17), an expression can be obtained for cm_z. It should be noted that V is a user inputted value in Surface Evolver. Equation (19) is the resulting equation.

$$cm_z = \left(\iint \frac{1}{2} z^2 \vec{k} \cdot d\vec{A}\right)/V \tag{19}$$

The process shown above is repeated to obtain the *x*-component, cm_x, and the *y*-component, cm_y, of the center of mass. The resulting equations are Eq. (20) and Eq. (21) with the unit vectors in the *x*-direction, $\vec{\imath}$, and *y*-direction, $\vec{\jmath}$.

$$cm_x = \left(\iint \frac{1}{2} x^2 \vec{\imath} \cdot d\vec{A}\right)/V \tag{20}$$

$$cm_y = \left(\iint \frac{1}{2} y^2 \vec{\jmath} \cdot d\vec{A}\right)/V \tag{21}$$

For the above equations to work, the entire liquid surface must be facetted, including the liquid-solid interface. The exception to this rule is when a tank wall is a flat surface at the $x = 0$, $y = 0$, and/or $z = 0$ planes for cm_x, cm_y, and/or cm_z, respectively. In these cases the walls at the zero plane can remain unfacetted and still give an accurate value for the center of mass, however, the rest of the walls should be facetted. The simulation will run faster by keeping the number of faces to a minimum, so keeping as many walls unfacetted as possible is recommended.

III. Results an Discussion

A. Zero Degree Contact Angle Results

The first set of results assumes design conditions for the GPM tank at launch. GPM's tank was designed to have a zero degree contact angle with hydrazine. The approximate fill fraction at launch is 70%. The initial position of the liquid propellant is varied to show how the hydrazine propellant would behave if the launch pushed the liquid to different regions of the tank. The initial propellant positions assumed that the PMD would have filled up, as per its design.

Figure 6 shows the final solution for the zero degree contact angle cases. The white bubbles represent the gas bubbles. The liquid propellant is wherever the bubble is not.

The initial position results shown in Fig. 6 give some interesting insight into the fluid behavior. First, the bubble will not automatically go back to the center of the tank. Instead, the bubble tends to remain near its initial position. Second, the final resulting bubble position does not dry out the PMD vanes, even if its initial position has it drying out some of the vane. Third, if the bubble touches the wall of the tank it will dry out a part of the tank wall. This third observation goes against the assumption that a perfectly wetting liquid will wet all the solid surfaces. The explanation for this can be found in Eq. (5). Equation (5) shows that it is not only the dry surface area, but also the free surface area, that contributes to the total energy in the problem. The combination of dry surface area and free surface area, found in cases where the bubble touches the wall, gives a solution where part of the wall is dried out. Fourth, the total energy is similar for cases where the bubble is completely wrapped around the center post, and where the gas bubble does not completely wrap around the center post. In flight, the second type of solution is more likely, because any significant acceleration would push the bubble away from the center post.

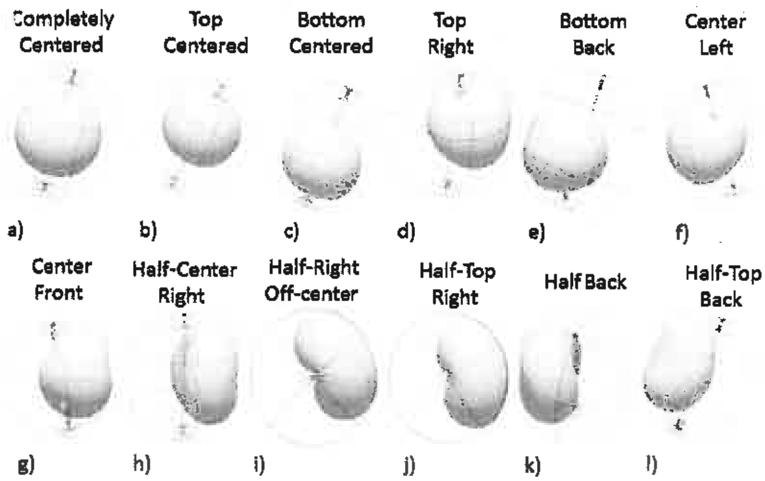

Figure 6. Liquid-gas interface results for zero degree contact angle cases at a fill fraction of approximately 70% with varying initial positions (see label above each subfigure for the initial position).

The results in Table 1 numerically confirm what we see in Fig. 6. As expected, the center of mass is offset more from the center of the tank if the bubble is not wrapped around the center post.

Table 1. Center of mass (CM) results in inches (in) for zero degree contact angle cases at a fill fraction of approximately 70% with varying initial positions.

Initial Bubble Position	Xcm (in)	Ycm (in)	Zcm (in)	CM Magnitude (in)
Completely Centered	0	0	0.01	0.01
Top-Center	0	0	-2.07	2.07
Bottom-Center	-0.03	0	2.17	2.17
Top-Right	0	-2.48	-1.81	3.07
Down-Back	2.48	0.05	1.73	3.02
Center-Left	0.01	2.63	0	2.63
Center-Front	-2.69	0	0.01	2.69
Half-Center-Right	0.16	-3.75	-0.09	3.75
Half-Right-Off-center	-1.17	-3.58	0.02	3.77
Half-Top-Right	-1.56	-3.36	-0.09	3.82
Half-Back	3.63	1.01	-0.03	3.77
Half-Top-Back	3.64	0.98	-0.40	3.79

B. Non-zero Degree Contact Angle with PMD

The third set of results examines the liquid propellant behavior in the GPM tank and PMD for varying fill fractions, contact angles, and initial positions. Throughout spacecraft operation, the fill fraction in the tank decreases and the position of the propellant changes. The contact angle changes when contamination enters the tank or propellant. Figure 7 shows the results with the liquid initial position being almost equal on the top and bottom of the tank. The fill fractions are varied between 3% and 70% and the contact angle is varied between 10 deg and 60 deg. The dark area represents the liquid position. The faces that break up the liquid-gas interface are transparent and so the darker areas within the shaded area show where the air bubble goes below the top most part of the liquid within the top or bottom liquid pools.

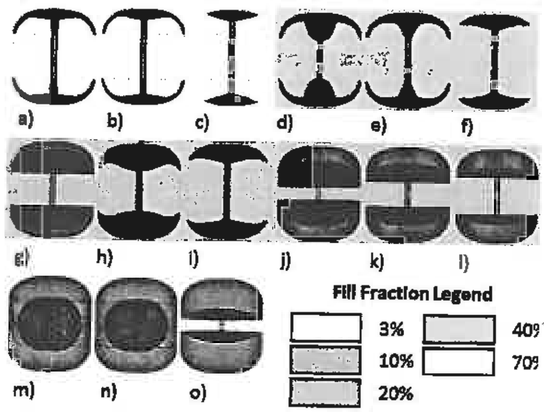

Figure 7. GPM tank and PMD liquid-gas interface case results with fluid equally distributed between top and bottom of tank, varying contact angles, where a) 10 deg, b) 30 deg, c) 60 deg, d) 10 deg, e) 30 deg, f) 60 deg, g) 10 deg, h) 30 deg, i) 60 deg, j) 10 deg, k) 30 deg, l) 60 deg, m) 10 deg, n) 30 deg, and o) 60 deg, and varying fill fractions (see legend).

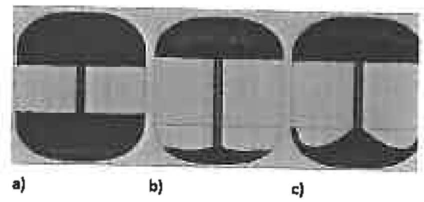

Figure 8. GPM Tank and PMD liquid-gas interface case results at a fill fraction of 20% and varying contact angles of a) 10 deg, b) 30 deg, c) 60 deg with more propellant initialized toward the top of the tank than at the bottom of the tank.

The results show two interesting trends. First, as the contact angle increases, the wetted surface area on both the vanes and tank wall decreases. Second, as the fill fraction increases, the region in which three-phase contact line occurs changes. These behaviors change the shape of the liquid gas interface and hence the location of the center of mass.

By initializing more liquid propellant at the top of the tank, the ability of the PMD to move the liquid to the outlet of the tank can be studied. Figure 8 shows the results at a fill fraction of 20%, with more propellant initialized at the top of the tank, and the contact angle varied from 10 deg to 60 deg.

Table 2. Center of mass (CM) results for non- zero degree contact angle cases at a fill fraction of approximately 20% with varying initial positions.

Contact Angle (deg)	Xcm (in)	Ycm (in)	Zcm (in)	CM Magnitude (in)
10	-0.01	1.35	-8.00	1.35
30	0.03	6.90	10.59	6.90
60	0.05	11.61	-18.00	11.61

Figure 8 shows that as the contact angle increases, the air bubble results are less centered about the center of the tank. Table 2 shows numerically these differences in center of mass location.

IV. Conclusions

Understanding how liquid propellant behaves in a low-gravity environment is important for the design of propellant tanks. Surface tension forces cause the liquid propellant to orient in unintuitive ways, thus changing the center of mass and the liquid-gas interface shape.

Surface Evolver can be used to model the liquid-gas interface shape and hence the center of mass location of the liquid propellant. The results in this report show that a complicated PMD and non-standard tank shaped tank, such as GPM's PMD and propellant tank, can be modeled for both non-zero and zero contact angle cases using Surface Evolver. The liquid-gas interface and hence the center of mass of the liquid propellant is affected by the liquid fill fraction, position of the liquid when thrusters (or other acceleration) is turned off, and the contact angle between the liquid propellant and the solid walls and vanes. As the contact angle decreases the liquid will wet more of the solid surfaces in the tank, but may not wet all the solid surface even at zero degree contact angle.

Future work in this area will include modifying Surface Evolver's wetted energy models and developing better face initializing techniques. This will enable higher fidelity results and more stable simulations.

Physical experiments are essential to showing that the Surface Evolver models are giving correct results. The microgravity experiments that could validate Surface Evolver include experiments done on parabolic flights, with drop-towers, with sub-orbital flights, or on-orbit flights.

Acknowledgments

This research was made possible by funding from NASA's Internal Research and Development (IRAD) Program, as well as the GPM Project. Special thanks go to Catilin Bacha for providing helpful feedback throughout the research and writing process.

References

[1]Surface Evolver, Software Package and Manual, Ver. 2.5, Ken A. Brakke, http://www.susqu.edu/brakke/evolver/evolver.html, 1992.

[2]Jaekle, D. E., Jr., "Propellant Management Device Conceptual Design and Analysis: Traps and Troughs," *31st AIAA/ASME/SAE/ASEE Joint Propulsion Conference and Exhibit*, AIAA, Washington, DC, 1995, pp. 1-13.

[3]Dominick, S. M., and Tegart, J. R., "Orbital Test Results of A Vaned Liquid Acquisition Device," *30th AIAA/ASME/SAE/ASEE Joint Propulsion Conference*, AIAA, Washington, DC, 1994, pp. 1-12.

[4]Aparicio, A., and Yendler, B., "Thermal Propellant Gauging at EOL, EuroStar 2000 Implementation," *SpaceOps 2008 Conference*, AIAA, Washington, DC, 2008, pp. 1-7.

[5]Weislogel, M. M., and Collicott, S. H., "Analysis of Tank PMD Rewetting Following Thrust Resettling," *40th AIAA Aerospace Sciences Meeting & Exhibit*, AIAA, Washington, DC, 2002, pp. 1-11.

[6]Collicott, S. H. and Weislogel, M. M., "Modeling of the Operatoin of the VTRE Propellant Management Device," *38th AIAA/ASME/SAE/ASEE Joint Propulsion Conference & Exhibit*, AIAA, Washington, DC, 2002, pp. 1-11.

[7]Rodriguez, E., and Collicott, S. H., "Mass Center Anomalies from Asymmetric Propellant Positions in Spacecraft," *44th AIAA Aerospace Sciences Meeting and Exhibit*, AIAA, Washington, DC, 2006, pp. 1-10.

[8]Brakke, K. A., "The Surface Evolver." *Experimental Mathematics*, Vol. 1, No. 2, 1992, pp 141-165.

[9]Collicott, S. H., and Weislogel, M. M., "Review of Surface Evolver Validation Tests for Zero-Gravity Fluids Applications," *41st Aerospace Sciences Meeting and Exhibit*, AIAA, Washington, DC, 2003, pp. 1-11.

[10]Chato, D. J., Marchetta, J., Hochstein, J. I. "Approaches to Validation of Models for Low Gravity Fluid Behavior," *42nd AIAA Aerospace Sciences Meeting and Exhibit*, AIAA, Washington, DC, 2004, pp. 1-15.

[11]Collicott, S. H., "Capillary Fluid Physics in Zero-Gravity," *41st AIAA Fluid Dynamics Conference and Exhibit*, AIAA, Washington, DC, 2011, pp. 1-12.

[12] Li, J., Chen, X., and Huang, Y., "The Review of Interior Corner Flow Research in Microgravity,"*Procedia Engineering*, Vol. 31, 2012, pp. 331-336.

[13]Tadmor, R., "Line Energy and the Relation between Advancing, Receding, and Young Contact Angles," *Langmuir*, Vol. 20, No. 18, 2004, pp. 7659-7664.

[14] Stewart, J., *Calculs: Early Transcedentals, 5th ed*, Brooks/Cole-Thomas Learning, Belmont, CA, 2003, Chap. 8.